Importance of the Gulf of Aqaba for the formation of bottom water in the Red Sea

Olaf Plähn,[1,2] Burkard Baschek,[3] Thomas H. Badewien,[1] Maren Walter,[4] and Monika Rhein[4]

Received 30 March 2000; revised 8 May 2001; accepted 13 September 2001; published 16 August 2002.

[1] Conductivity-temperature-depth tracer and direct current measurements collected in the northern Red Sea in February and March 1999 are used to study the formation of deep and bottom water in that region. Historical data showed that open ocean convection in the Red Sea can contribute to the renewal of intermediate or deep water but cannot ventilate the bottom water. The observations in 1999 showed no evidence for open ocean convection in the Red Sea during the winter 1998/1999. The overflow water from the Gulf of Aqaba was found to be the densest water mass in the northern Red Sea. An anomaly of the chlorofluorocarbon component CFC-12 observed in the Gulf of Aqaba and at the bottom of the Red Sea suggests a strong contribution of this water mass to the renewal of bottom water in the Red Sea. The CFC data obtained during this cruise are the first available for this region. Because of the new signal, it is possible for the first time to subdivide the deep water column into deep and bottom water in the northern Red Sea. The available data set also shows that the outflow water from the Gulf of Suez is not dense enough to reach down to the bottom of the Red Sea but was found about 250 m above the bottom. *INDEX TERMS:* 4875 Oceanography: Biological and Chemical: Trace elements; 4283 Oceanography: General: Water masses; 4243 Oceanography: General: Marginal and semienclosed seas; 4271 Oceanography: General: Physical and chemical properties of seawater; *KEYWORDS:* Gulf of Aqaba, Red Sea, formation of bottom water, tracer oceanography, CFC, overflow

1. Introduction

[2] The Red Sea Water (RSW) is one of the most important intermediate water masses in the Indian Ocean, being a major source of warm and highly saline water in the interior of the ocean [e.g., *Düing and Schwill*, 1967]. RSW spreads from the Red Sea into the Arabian Sea and moves southward along the African coast. It has been observed as far south as the retroflection region of the Agulhas Current [*Fine et al.*, 1988]. The spreading of RSW in the Indian Ocean has been studied by using the salinity signal of the water mass [e.g., *Gamsakhurdiya et al.*, 1991]. However, the formation of the water mass in the northern Red Sea still raises some questions.

[3] *Wyrtki* [1974] proposed three different sources for the formation of RSW: overflow from the Gulf of Aqaba through the Strait of Tiran, inflow from the Gulf of Suez, and open ocean convection in the northern Red Sea. *Cember* [1988] pointed out that deep convection in the open northern Red Sea has never been directly observed. He suggested that overflow water from the Gulf of Aqaba and open ocean convection in February/March south of the Sinai peninsula are both important for the deep water formation in the Red Sea. In contradiction, *Neumann and Gill* [1962] supposed that the Strait of Tiran would be a barrier that cuts off the Gulf of Aqaba from the circulation in the Red Sea. *Woelk and Quadfasel* [1996] showed that plume convection from the Gulf of Suez alone can explain the observed change in the deep water characteristics in 1982/1983. All these analyses are based on hydrographic data that were measured 10–30 years ago. This study presents more recent hydrographic, velocity, and chlorofluorocarbon (CFC components CFC-11 and CFC-12) measurements from the northern Red Sea and Gulf of Aqaba collected in February and March 1999 (Figure 1). The new data set makes it also possible to separate the deep water column into deep and bottom water.

2. Data

[4] The data analyzed in this study were collected during R/V *Meteor* cruise M44/2 (21 February to 7 March 1999). The roman numbers (I–XII) in Figure 1 represent the position of the measurements. All of these stations were repeated at least three times during the cruise.

[5] Temperature and salinity profiles were obtained with a conductivity-temperature-depth system (LTO, model Neil Brown Mark IIIb). The temperature and pressure sensors were calibrated in the laboratory before the expedition and were verified by reversing thermometers. The conductivity cell was calibrated from salinity bottle samples. The accuracy in temperature is estimated to be <0.015°C, and the

[1]Institut für Meereskunde, Universität Kiel, Kiel, Germany.
[2]Also at Institut für Ostseeforschung Warnemünde, Universität Rostock, Rostock, Germany.
[3]Institute of Ocean Sciences, Sidney, British Columbia, Canada.
[4]Institut für Umweltphysik, Universität Bremen, Bremen, Germany.

0148-0227/02/2000JC000342

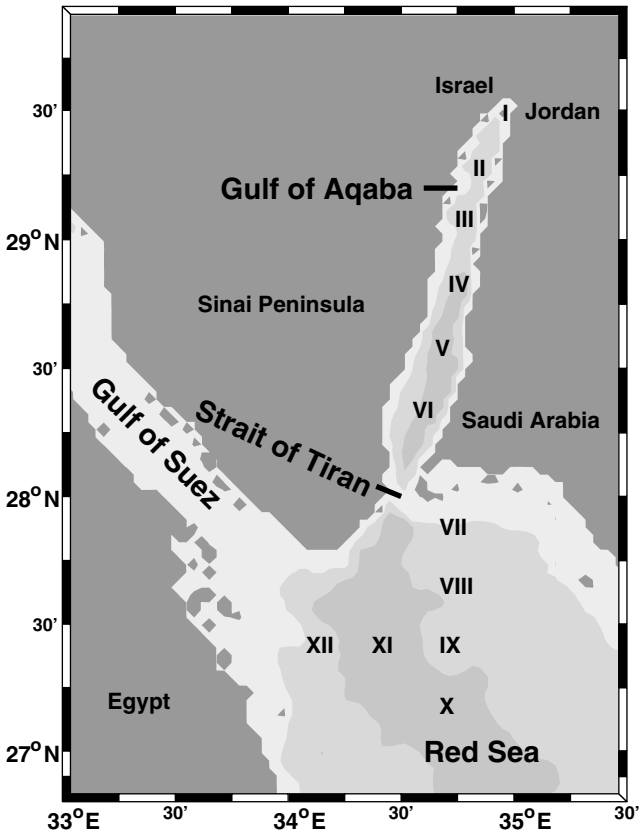

Figure 1. Positions of the hydrographic stations (marked by roman numbers) during R/V *Meteor* cruise M44/2 (21 February to 7 March 1999) in the Gulf of Aqaba and the northern Red Sea.

accuracy in salinity is 0.004. The data of the vessel-mounted thermosalinograph (Seacat) were calibrated from water samples and the CTD data.

[6] Chlorofluorocarbons (CFCs) were collected using precleaned 10 L Niskin bottles mounted on the CTD unit. Both components (CFC-11 and CFC-12) were measured on board with a gas chromatographic technique described by *Bullister and Weiss* [1988]. The precision was checked by analyzing 15% of the water samples twice; the mean rms of the difference between dublicates was 0.65% for CFC-12 and 0.85% for CFC-11. The CFC data obtained during this cruise are the first available for this region.

[7] Direct velocity measurements were made with a 150 kHz narrowband vessel-mounted acoustic Doppler current profiler (ADCP) with a beam angle of 30°. The ensemble length was 2 min, and the bin length was 8 m. For navigation, a Global Navigation Satellite System (GLONASS)/GPS receiver was used for the correction of the ships motion and oscillations of the gyro compass (Schuler oscillations).

[8] The research activities during the *Meteor* cruise were restricted by the governments of Saudi Arabia and Egypt. It was not permitted to collect any data in the territorial waters of Saudi Arabia. Twenty nautical miles north and south of the Strait of Tiran and in the Gulf of Suez, only underway measurements with vessel-mounted acoustic Doppler current profiler (ADCP) and thermosalinograph were allowed. Therefore a detailed study of the hydrography in the Strait of Tiran was impossible as were direct measurements of the outflow from the Gulf of Suez. The data collected during R/V *Meteor* cruise M44/2 were compared to historical data from National Oceanographic Data Centre (NODC) to study the temporal variability of the deep water formation. Most of the historical data was obtained with bottle samplers, measured more than 30 years ago.

3. Observations in the Northern Red Sea

[9] The contributions of the dense inflow from the Gulf of Aqaba and the Gulf of Suez as well as the open ocean convection to the renewal of the deep water masses are studied separately using new observations and historical data. Before analyzing the significance of each of these sources the hydrographic and tracer data collected in the northern Red Sea during M44/2 are presented. The following figures represent the mean hydrography and the tracer fields, observed in February and March 1999. The variability during this period was negligible in the whole region, except of the strong vertical oscillations of the thermocline in the Gulf of Aqaba, which are unimportant for the study of the deep water formation in the Red Sea.

3.1. Zonal Sections of CFC and Salinity

[10] Usually, CFCs are introduced into the oceanic mixed layer by air-sea gas exchange. If CFC is transfered into the deep ocean only by vertical diffusion, the concentrations decrease exponentially with depth, as observed in the Arabian Sea by *Rhein et al.* [1997]. High CFC concentrations in the deep water are mainly caused by deep convection, which are then further advected by (boundary) currents.

[11] Figure 2 shows the CFC-12 saturation along the 27.5°N section (stations IX, XI, and XII, see Figure 1). The saturation at the sea surface is nearly 100% and decreases with depth. Along this section both CFC components reach a minimum at about 500 m depth and increase again toward the bottom. The CFC maximum close to the bottom (beneath the isopycnal $\sigma_\theta = 28.59$), with saturation of more than 70%, indicates that deep water has been recently formed in the northern Red Sea or has its source in the dense outflow from the Gulf of Aqaba or the Gulf of Suez.

[12] It is unlikely that this maximum is caused by recent open ocean convection in the northern Red Sea since the concentration minimum at intermediate depths would have been eroded by the convection processes. This is also supported by the observed stable density stratification of the water column, increasing from $\sigma_\theta = 28.2$ to $\sigma_\theta = 28.6$ (Figure 2). Because the measurements were made in February and March (the coldest time of the year, when convection usually happens) and air temperatures increased at the end of the cruise, open ocean convection seems to be unlikely also for rest of the year.

[13] The salinity along the 27.5°N section (Figure 3) increases toward the bottom from 40.2 to more than 40.5, which is in agreement with the observations of *Woelk and Quadfasel* [1996]. The largest values were found in the western part of the northern Red Sea. In detail, there are two local maxima, the upper one at about 450 m depth and the deeper one at 900 m depth.

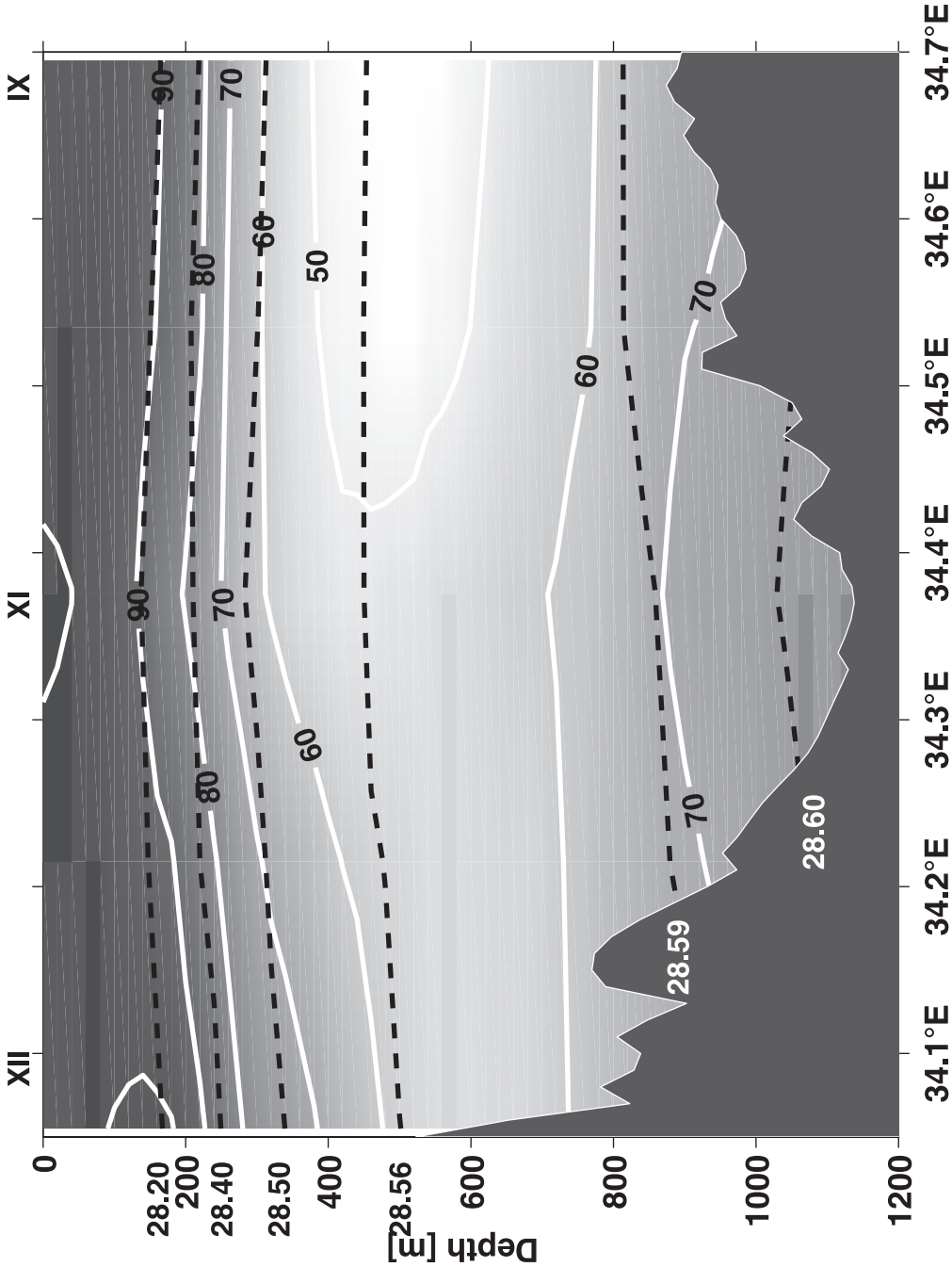

Figure 2. CFC-12 saturation (percent) and density (σ_θ, dotted lines) in the northern Red Sea along the 27.5°N section (stations IX, XI, and XII).

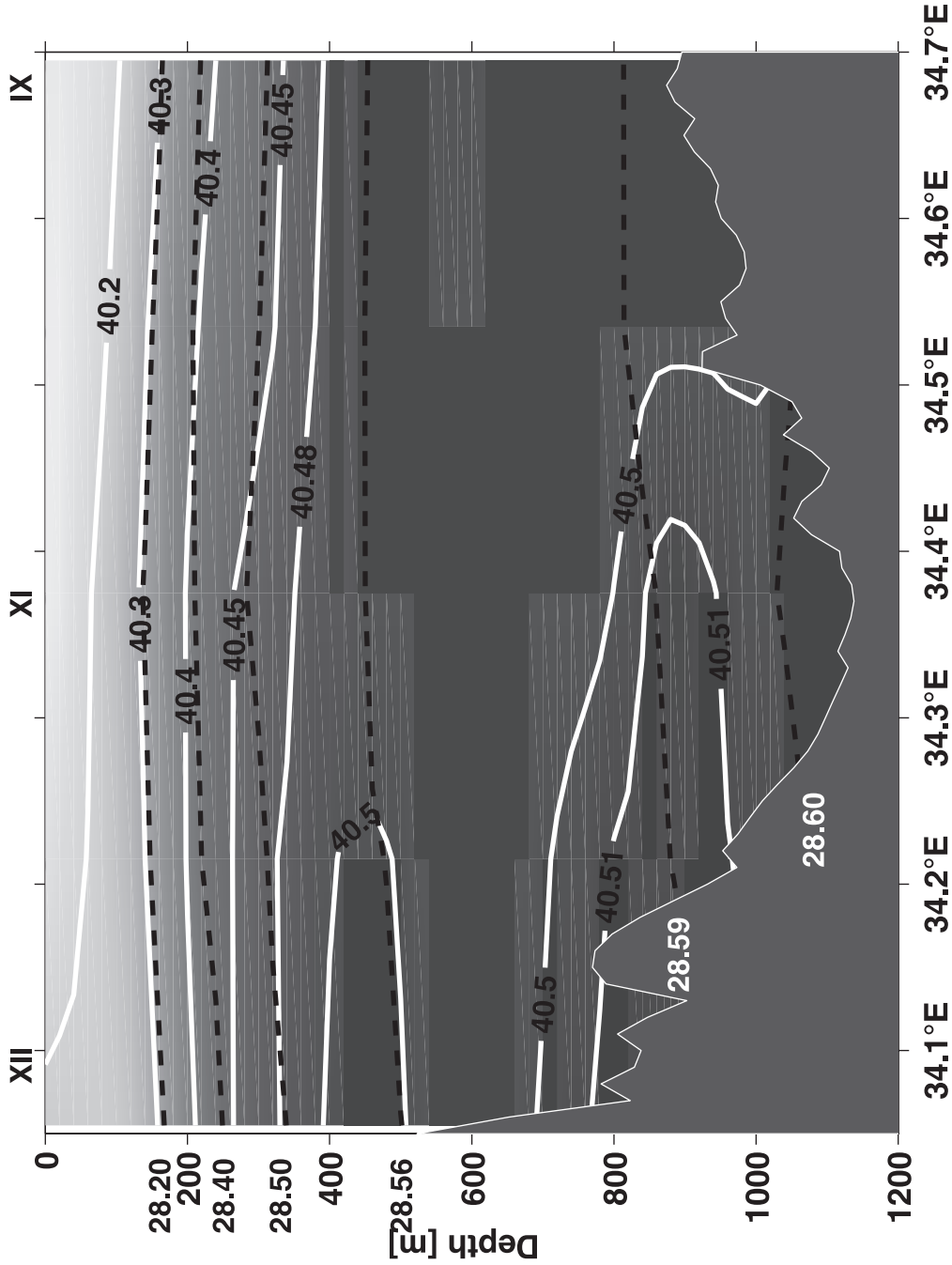

Figure 3. Salinity and density (σ_θ, dotted lines) in the northern Red Sea along the 27.5°N section (stations IX, XI, and XII).

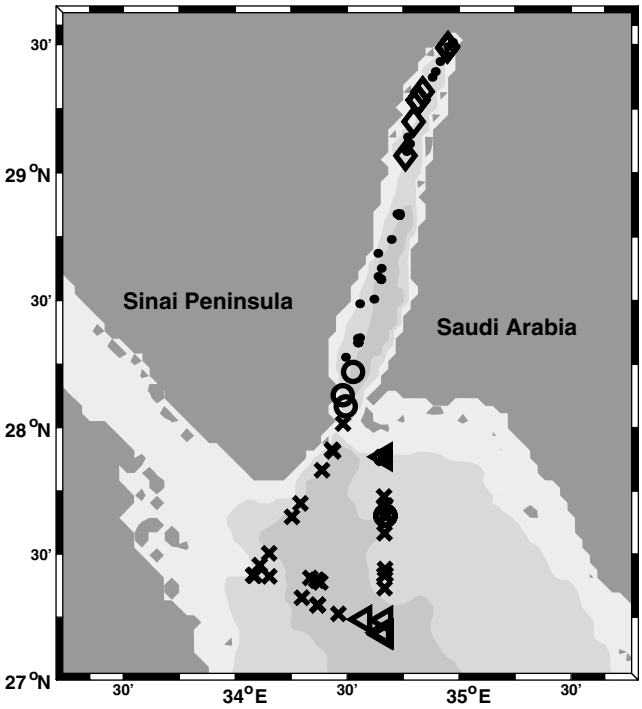

Figure 4. Density at the sea surface; $\sigma_\theta \geq 28.7$ (diamond), $28.7 > \sigma_\theta \geq 28.4$ (dot), $28.4 > \sigma_\theta \geq 28.1$ (circle), $28.1 > \sigma_\theta \geq 27.8$ (cross), and $27.8 > \sigma_\theta$ (triangle). The density was calculated from SST and salinity continuously measured during cruise M44/2 with a vessel-mounted thermosalinograph.

[14] However, the salinity and CFC extrema are located at different depths. While the CFC maximum has no zonal gradient and was found at the bottom (Figure 2), the deep salinity maximum is located 250 m above the bottom (Figure 3). On the other hand, the CFC minimum observed between 400 and 600 m depth is more pronounced at the western side of the section (which ended in the center of the Red Sea) and is not characterized by a salinity signal, which suggests that the deep CFC and salinity maxima originate from different sources.

3.2. Sea Surface Measurements

[15] Although open ocean convection is very unlikely in 1999, the cold northerly winds might induce shelf convection south of the Sinai peninsula. Observations in that region were restricted because of political reasons, only allowing underway measurements with the thermosalinograph. These data were used to calculate the surface density presented in Figure 4 in order to estimate the possibility of shelf convection. During cruise M44/2 the surface density was $\sigma_\theta = <28.1$ along the southern coast of Sinai. Since the density at the bottom reaches up to $\sigma_\theta = 28.6$ (Figure 2), shelf convection can also be excluded as a possible source for the bottom water during winter 1998/1999. In February/March 1999 the temperature at 400 m depth was 21.5°C and was <21.3°C at the bottom. This is consistent with *Woelk and Quadfasel* [1996], who observed a mean temperature at about 400 m depth between 21.5° (May 1983) and 21.7°C (October 1982) and temperatures between 21.3° (May 1983) and 21.6°C (October 1982) at the bottom. Taking into account that the salinity increases at least by 0.2 from the surface toward the bottom (Figure 3) [*Woelk and Quadfasel*, 1996] and assuming that the water mass properties of the deeper ocean are relatively steady, the surface temperature had to be colder than 21.3°C for deep convection to occur. Figure 5 shows the NODC sea surface temperatures (SST) collected in different years with expendable bathy thermograph (XBT) measurements or with bottle samplers near the southern edge of Sinai. The lowest SST of 22.0°C was observed in March 1959. The accuracy of the data set is unknown; the standard deviation of the horizontal variability is about 0.2–0.5°C. Since the lowest SST was found to be 22.0°C (Figure 5), a complete mixing of the water column down to the bottom seems to be very unlikely. This result is also supported by *Cember* [1988], who pointed out that open ocean convection in the northern Red Sea has never been directly observed and does not account for the total rate of convective deep water formation. However, convection down to intermediate depths might be possible in some cold winters.

[16] The results show that the observed high CFC concentrations near the bottom of the Red Sea (Figure 2) cannot be caused by convection in the northern Red Sea, suggesting that a well-ventilated water mass was advected into that region. Therefore the outflow waters from the Gulf of Suez and the Gulf of Aqaba will be studied in the next sections as further possible sources of the bottom water in the Red Sea.

4. Gulf of Suez

[17] The Gulf of Suez is a semienclosed shallow basin (≈25–40 km width and ≈290 km length) located in the northwest of the Red Sea (Figure 1). The mean water depth is 50–70 m. The connection to the Red Sea at the southern end of the gulf is not constricted by a narrow sill, and the water depth increases rapidly to more than 1000 m depth in the Red Sea.

[18] The published transports of outflow water from the Gulf of Suez (GSW) are between 0.025 Sv [*Soliman*, 1995] and 0.12–0.17 Sv [*Woelk and Quadfasel*, 1996] (1 Sv = 10^6 m^3 s^{-1}). The maximum describes the upper boundary limited by the condition of maximal exchange.

[19] The historical data collected at about 28°N (Figure 6) during different months show a strong seasonal cycle. Because of high temperatures in summer, the density in the Gulf of Suez reaches only $\sigma_\theta = 28.0$. Thus, in summer the GSW cannot contribute to the formation of ventilated deep or bottom water in the Red Sea, which is supported by *Cember* [1988], who published temperature and salinity characteristics of the Red Sea, the Gulf of Suez, and the Gulf of Aqaba.

[20] During winter, dry and cold continental winds intensify cooling and evaporation and increase the density at the surface in the gulf, reaching $\sigma_\theta > 29.0$ (Figure 6; circle and asterisk). This indicates that only in winter the density of the outflow water is large enough to reach depths close to the bottom of the Red Sea.

[21] *Maillard* [1974] compared direct current measurements and hydrographic data of the outflow of GSW. The author assumed that new deep water is a mixture of GSW and water located in the northern Red Sea between 30 and 75 m depth. During a cruise in February 1963 she found in the

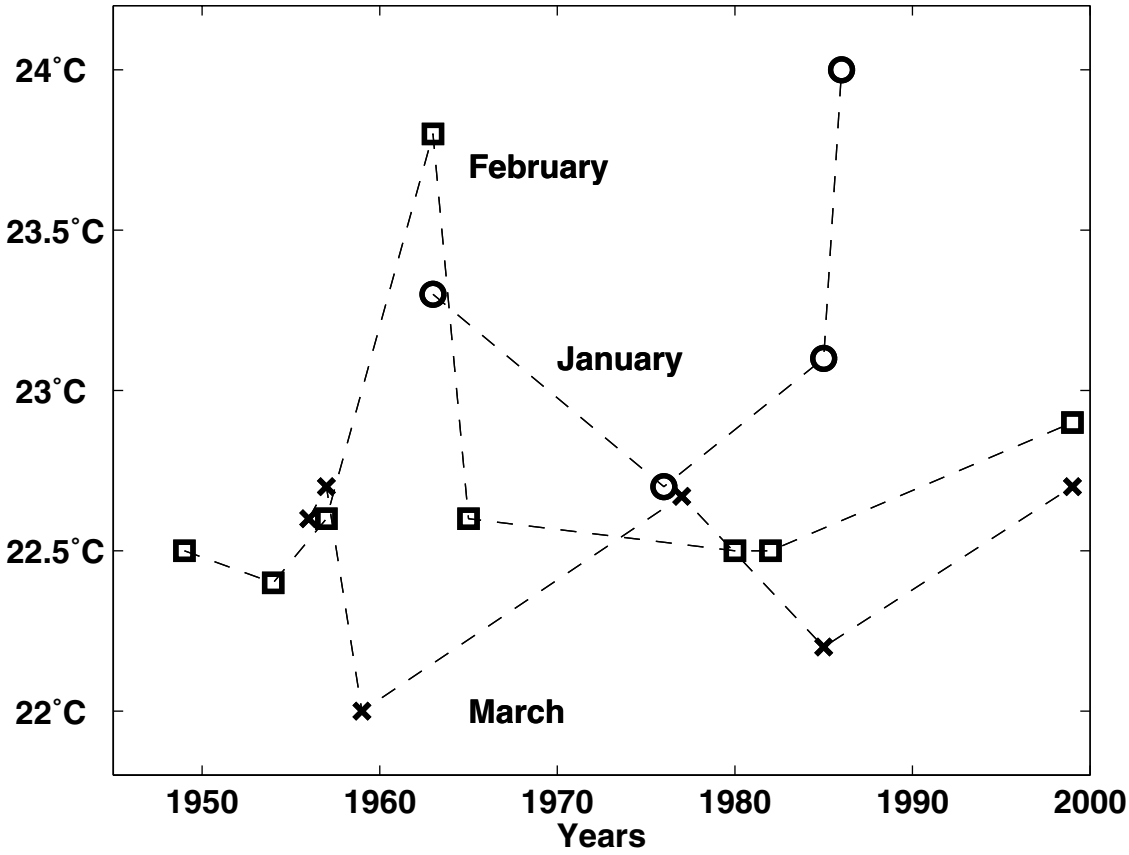

Figure 5. SSTs measured in different years in January (circle), February (square), and March (cross) near the southern edge of the Sinai peninsula.

northern Gulf of Suez a density of more than $\sigma_\theta \geq 29.0$ (Figure 6). However, at the southern end of the gulf the author only found water lighter than $\sigma_\theta = 28.6$ (Figure 7). This is in agreement with other observations made in different years and also with the data collected in February/March 1999.

[22] None of the density profiles measured at the slope between the southern exit of the shallow Gulf of Suez and the Red Sea during that time exceeded densities of $\sigma_\theta = 28.6$. Values as high as this are only present in the deep Red Sea (Figure 7; circle). Since the density in the Gulf of Suez is much higher some miles farther north (Figure 6), strong mixing with inflowing water from the Red Sea must have diluted the dense water or the core of the dense outflow must have spread along the Egyptian coast into the Red Sea and was therefore not observed.

[23] Surprisingly, the available data (Figure 7) from the slope toward the Red Sea do not reflect the extreme dense water observed in the Gulf of Suez (Figure 6). Thus the GSW cannot cause the CFC maximum observed at the bottom of the Red Sea (Figure 2) but might be responsible for the deep salinity maximum measured on the western side of the 27.5°N section at about 900 m depth (Figure 3).

[24] However, it might be possible that sometimes a plume of dense water leaves the shallow Gulf of Suez. This theory is supported by *Woelk and Quadfasel* [1996], who mentioned that plume convection from the Gulf of Suez might happen every 4–7 years. The authors did not observe such an event directly but concluded their results from changes in the deep water characteristics in the Red Sea in comparison with meteorological time series. They published the annual mean surface temperature in the Gulf of Suez averaged from November to April between the years 1945 and 1992. The winter 1982/1983, subject of their study, is one of the coldest of the observed time series. If the SST is not as cold as in winter 1982/1983, the density is lower, and the contribution of GSW might be weaker than at that time.

[25] However, their model results showed that plume convection only renews the water column between 450 and 1000 m depth. Below 1000 m depth, the level of the bottom water, their calculations show no significant transport, which supports the assumption that GSW outflow does not form bottom water in the Red Sea.

5. Gulf of Aqaba

[26] The Gulf of Aqaba is a deep and narrow basin in the northeast of the Red Sea (Figure 1). This semienclosed gulf is about 180 km long and 14 km wide and reaches a depth of up to 1800 m. In the south it is connected to the Red Sea by the narrow (≈2 km width) Strait of Tiran. In detail the strait consists of two passages [*Hall*, 1975], the deep (≈260 m) Enterprise Passage on the western end of the sill (≈1.2 km width) and the shallow (≈75 m deep) Grafton Passage to the east (≈0.9 km width).

[27] The Gulf of Aqaba is zonally bounded by high desert mountains that steer the wind along the main axis. In winter

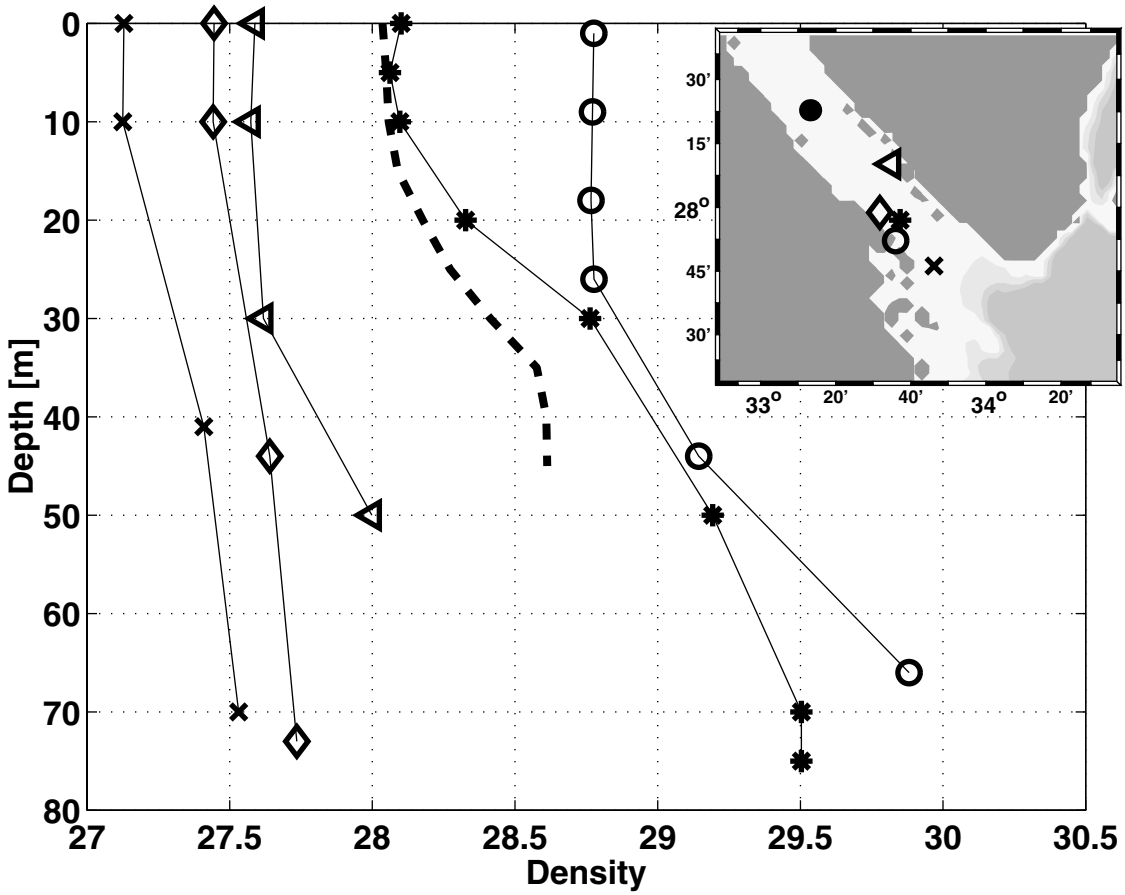

Figure 6. Density profiles in the Gulf of Suez near 28°N measured in October 1923 (NODC; triangle), September 1962 (NODC; diamond and cross), February 1963 (R/V *Giraud*; asterisk), February 1965 (R/V *Atlantis*; circle), and October 1982 (R/V *Marion Dufresne*; dotted line).

a cold southward wind cools off the surface water and forces a strong surface mixing, especially in the northern part of the gulf. The climate is arid with a yearly average net evaporation of 0.01 m d^{-1} [*Murray et al.*, 1984]. Previous investigations at the sill of the Strait of Tiran [e.g., *Klinker et al.*, 1976] showed that despite of the southward wind forcing, there is a northward inflow of low-salinity surface water from the Red Sea. Below 120 m the high-saline Gulf of Aqaba Water (GAW) flows southward into the Red Sea.

[28] *Murray et al.* [1984] measured with moored current meters along-strait velocities of ±0.5 m s^{-1} in both layers during a period from February to March 1982 and calculated an outflow transport of about 0.03 Sv through the Enterprise Passage. The authors also found the σ_θ = 28.6 isopycnal at about 90 m depth in the center of the strait, deepening to the south. They supported the observations from *Hecht and Anati* [1983] that the density of the GAW outflow is between σ_θ = 28.6 and σ_θ = 28.75. *Murray et al.* [1984] also pointed out that the dense outflow water cannot enter the Red Sea through the shallow Grafton Passage. Therefore this passage is neglected in the following.

5.1. Hydrography and Tracer Distributions

[29] The meridional distributions of temperature (Figure 8) and salinity (Figure 9) measured in February and March 1999 show only small vertical and horizontal gradients. In the upper 400 m the salinity increases northward from <40.45 to >40.63, and the temperature decreases from >21.7°C to about 21.4°C. At about 400 m depth the data show a salinity minimum (at $\sigma_\theta \approx 28.8$) in the northern part of the gulf (Figure 9). From summer to fall of 1988 and 1989, *Wolf-Vecht et al.* [1992] also observed a salinity minimum in this region. However, this minimum was located at about 100 m depth in summer; it deepens as the mixed layer deepens in fall to about 200 m depth and is eroded by mixing processes. The authors assumed that the only source of the near-surface minimum can be an inflow of fresher RSW. The density of the salinity minimum measured in winter 1999 is about σ_θ = 28.8, and the salinity is more than 40.57. Both values are much higher than observations near the surface of the Red Sea during cruise M44/2 (Figure 3). Neither *Klinker et al.* [1976] nor *Wolf-Vecht et al.* [1992] observed such a salinity minimum at 400 m depth in the Gulf of Aqaba. The high values of the CFC-11 saturation over the whole water column in the Gulf of Aqaba (Figure 10) indicate the strong vertical mixing in the entire basin, as the CFC-11 saturation is more than 90% even at the density range of the outflow water.

[30] The CFC-12 component shows a contamination signal in the gulf (Figure 11). The core of this contamination was found at about 500 m depth, with saturation larger than 250% relative to the concentration in the atmosphere. The

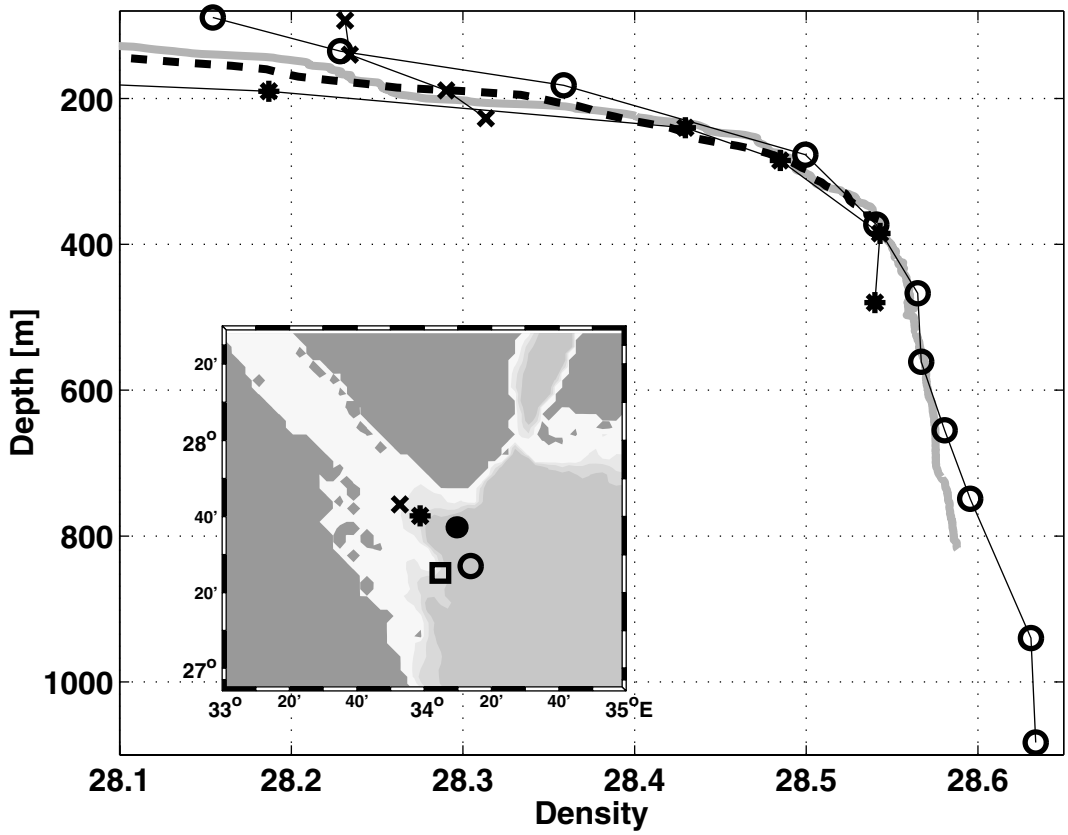

Figure 7. Density profiles at the southern end of the Gulf of Suez measured in February 1963 (R/V *Giraud*; asterisk), February 1965 (R/V *Atlantis*; circle and cross), October 1982 (R/V *Marion Dufresne*; dotted line), and February 1999 (R/V *Meteor*; shaded line and square).

highest concentrations are found in the northern part of the gulf. These extremely high values cannot be created by air-sea gas exchange since the sea surface concentrations everywhere are close to equilibrium with the atmospheric values. The source and the temporal input function of this contamination is still unknown. A link to the described salinity minimum might be possible but could not be proved. A section across the gulf shows a small increase of this contamination maximum toward the eastern side, indicating that this anomaly originates presumably in the industrial regions of Jordan or Saudi Arabia.

[31] Such a contamination signal is a rare event, but it is not an unique case. In the Persian Gulf outflow water a similar CFC-12 anomaly was observed in the Gulf of Oman by *Rhein et al.* [1997] and in the northern Arabian Sea near the island of Socotra by *Plähn et al.* [1999]. It is likely that the source of the high CFC concentrations observed at the bottom of the Red Sea (Figure 2) is the dense overflow of GAW. The density at the bottom of the Red Sea was found to be about $\sigma_\theta = 28.6$, and the density of the overflow water in the Strait of Tiran is about $\sigma_\theta = 26.6-26.75$ [*Hecht and Anati*, 1983; *Murray et al.*, 1984]. Within this density range of $\sigma_\theta = 26.6-26.75$ the CFC-12 saturation in the southern end of the Gulf of Aqaba (station VI, Figure 1) is about 105–120% (Figure 12), while the CFC-11 saturation shows a nearly homogeneous distribution of 95–100%. Since the southernmost measurements in the gulf were carried out 20 nm north of the Strait of Tiran, it is likely that mixing processes will further modify the CFC-12 anomaly on the way toward the Red Sea. However, if the GAW outflow contributes significantly to the renewal of the bottom water in the Red Sea, the contamination signal should also be recognizable there in the CFC maximum at the bottom (Figure 2).

[32] In the Red Sea the saturation profiles of CFC-11 and CFC-12 are very similar in the upper 900 m (Figure 13). At greater depth, between 900 m and the bottom, CFC-11 is relatively constant, but the CFC-12 concentration increases significantly farther toward the bottom. There the mean CFC-12 saturation is by 5% higher than the CFC-11 value. Table 1 summarized the CFC-11/CFC-12 saturation ratio observed below $\sigma_\theta = 28.60$. At station XII and IX the density was not reached; thus the values at the bottom are shown there. The lowest ratios are measured at stations XI and X. Because of their location (see Figure 1), only a sparse signal was observed at stations VII and VIII. The main part of the dense GAW reached the Red Sea west of stations VII and VIII.

5.2. Box Model

[33] Usually, both CFC components have about the same saturation relative to the atmosphere. The discrepancy between the saturations of both components in about 500 m depth in the Gulf of Aqaba (Figure 12) and in the bottom water of the Red Sea is unusual and leads to the conclusion that GAW is contributing to the formation of

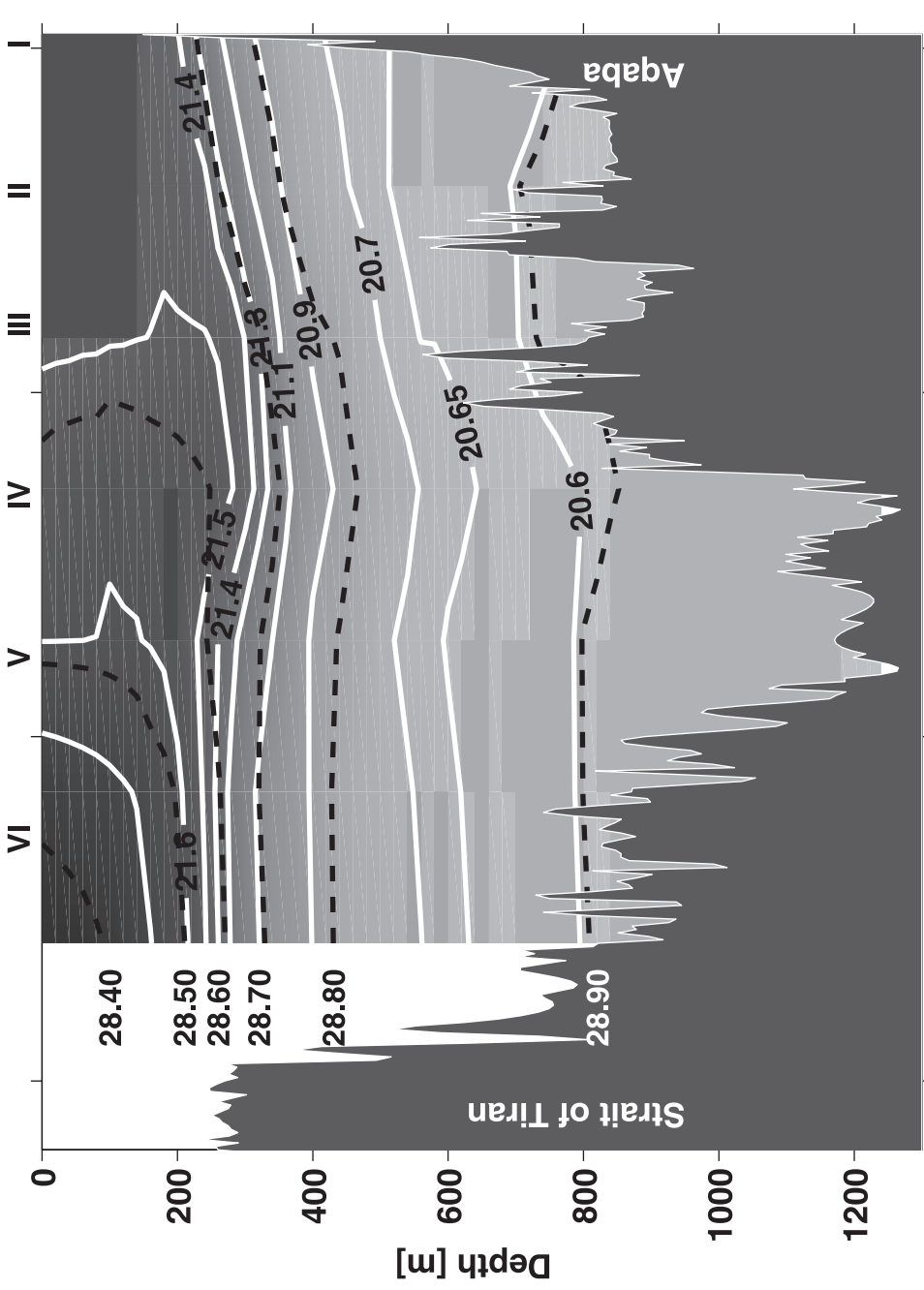

Figure 8. Temperature (°C) and density (σ_θ, dotted lines) in the Gulf of Aqaba measured at CTD stations I–VI during cruise M44/2.

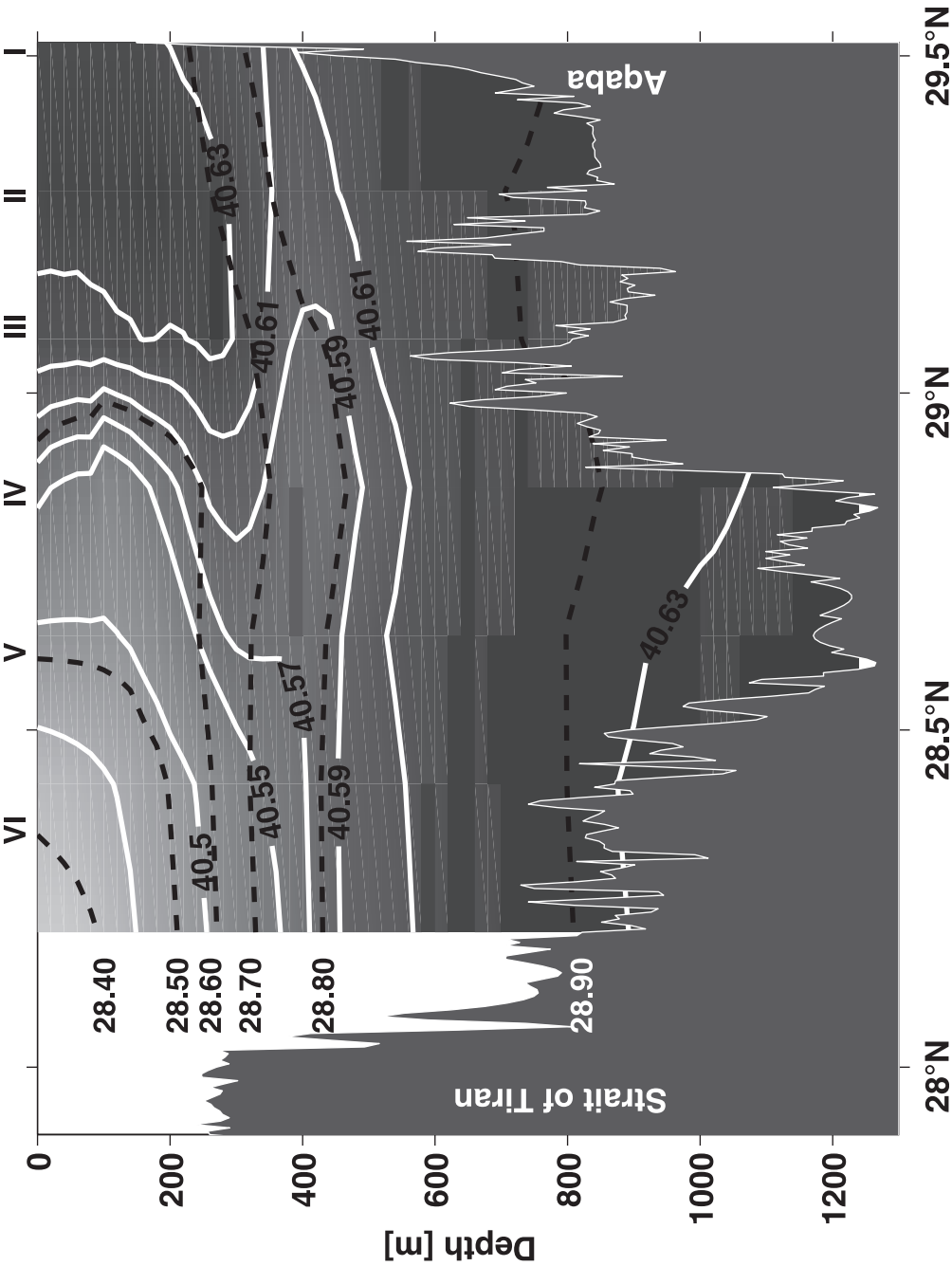

Figure 9. Salinity and density (σ_θ, dotted lines) in the Gulf of Aqaba measured at CTD stations I–VI during cruise M44/2.

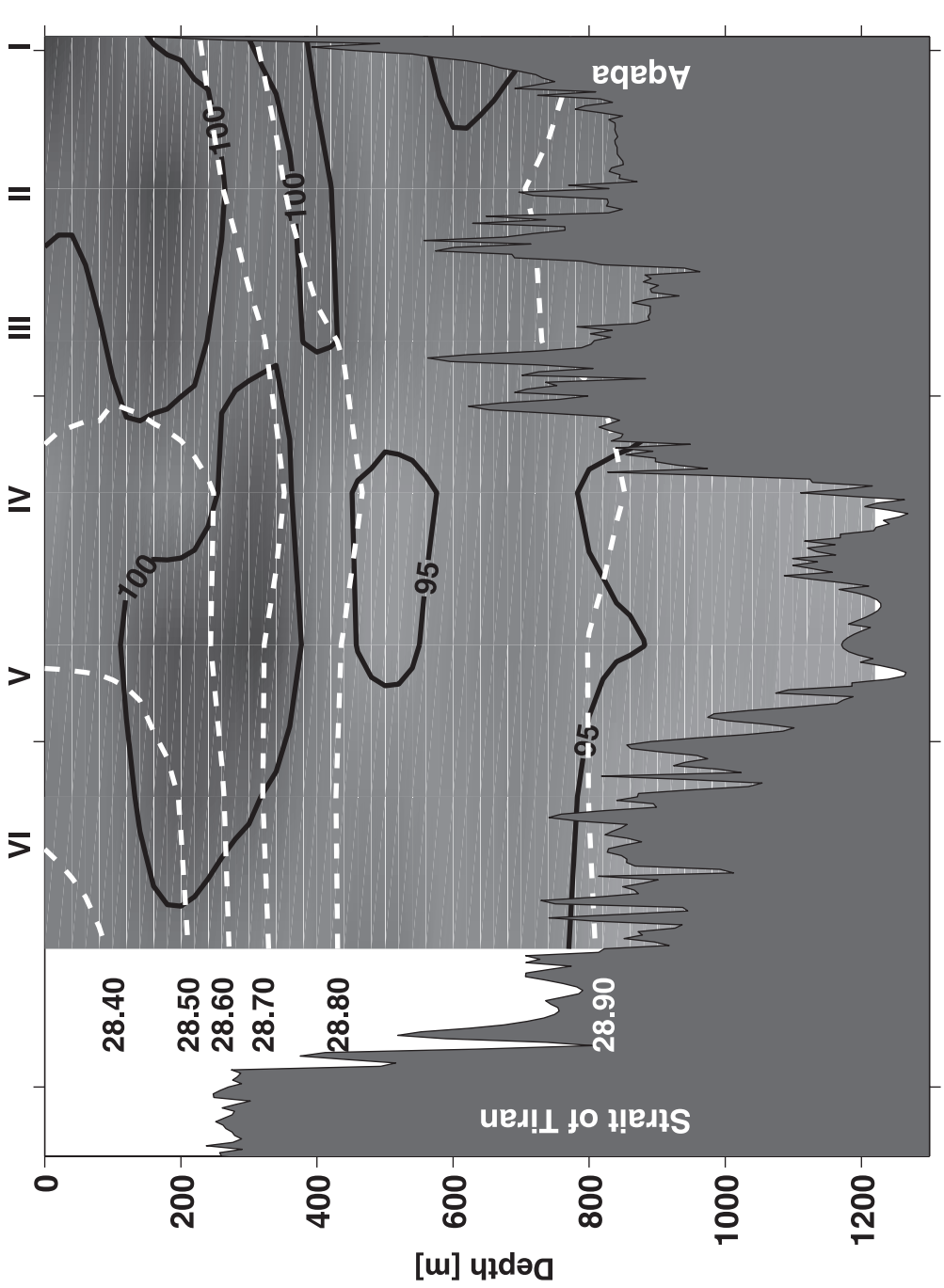

Figure 10. CFC-11 saturation and density (dotted lines) in the Gulf of Aqaba measured at CTD stations I–VI during cruise M44/2.

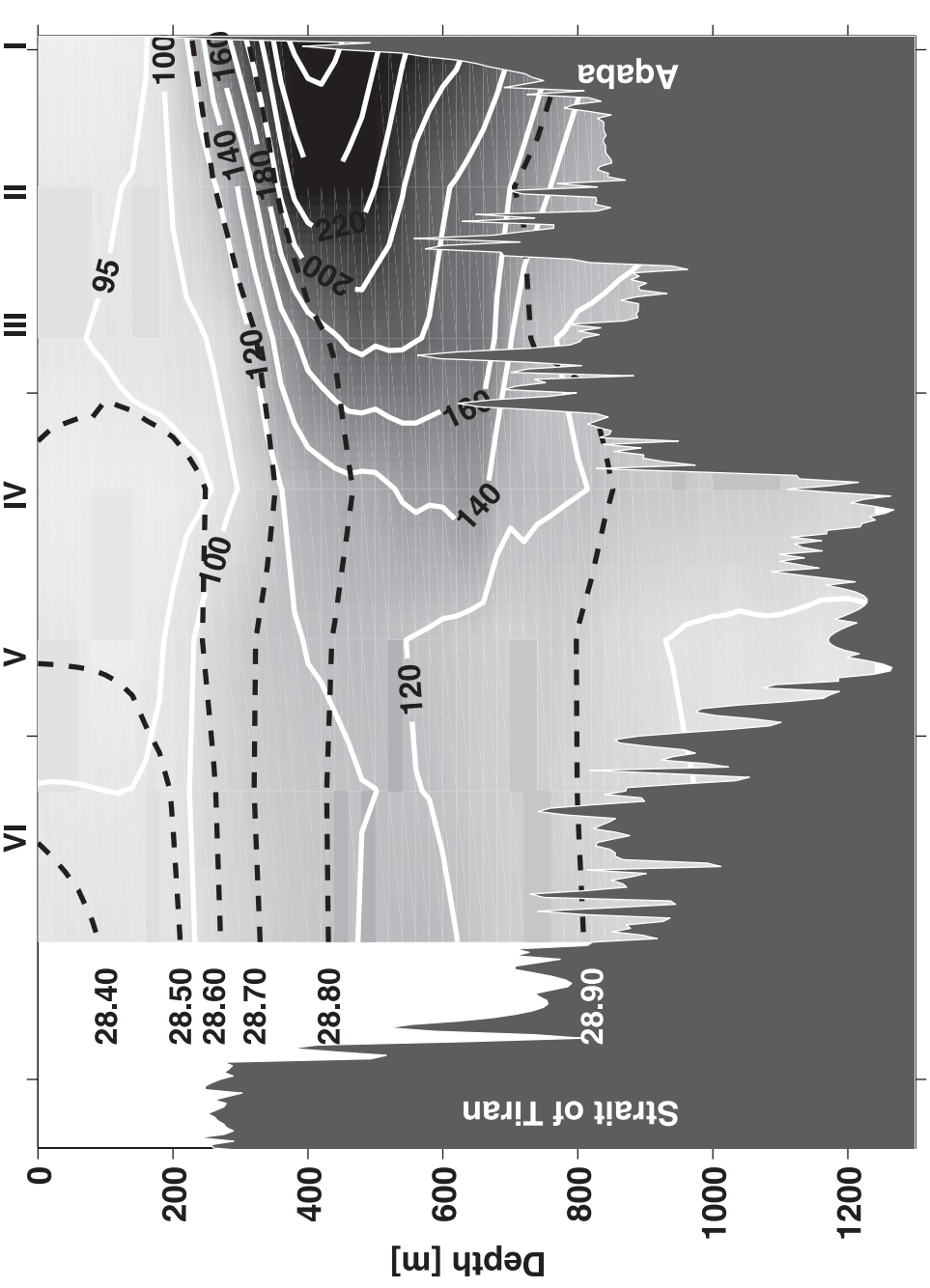

Figure 11. CFC-12 saturation and density (dotted lines) in the Gulf of Aqaba measured at CTD stations I–VI during cruise M44/2.

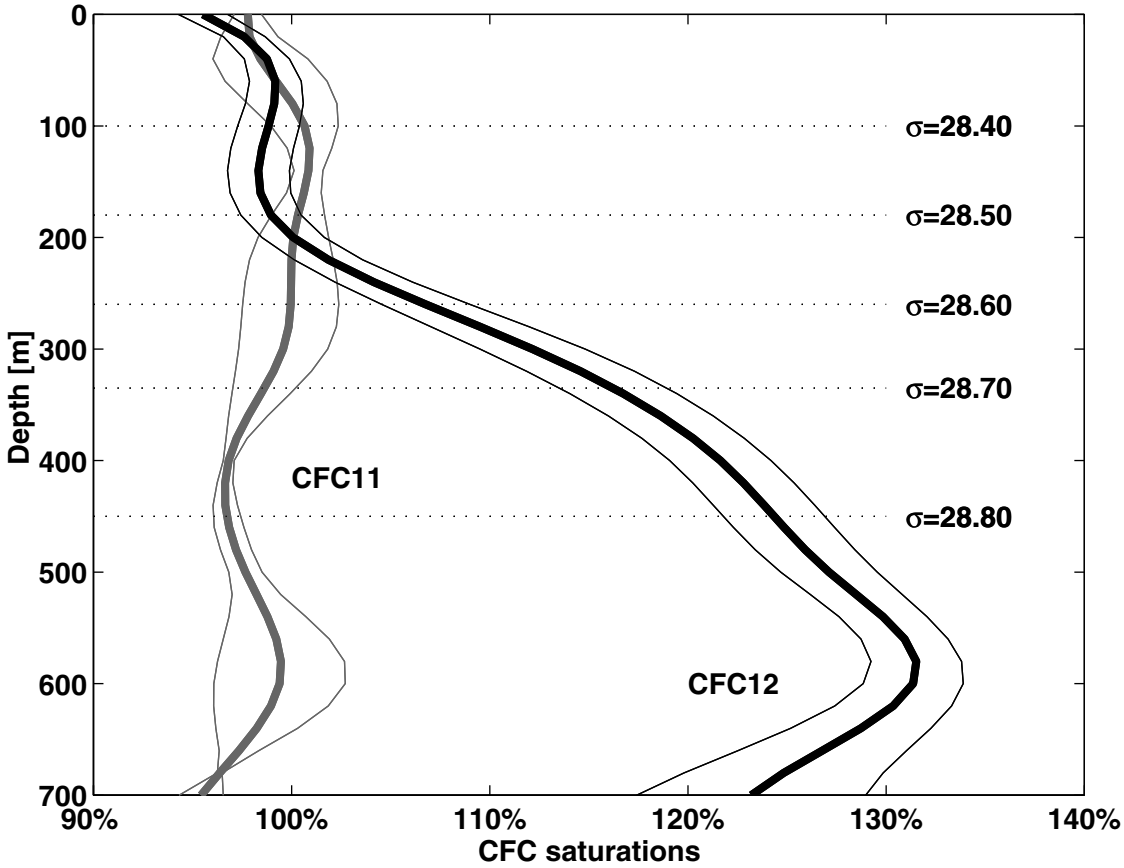

Figure 12. Profiles of the mean CFC saturations (bold lines) measured four times in the southern part of the Gulf of Aqaba (station VI). The thin lines represent the standard deviation. The dotted lines indicate the isopycnals.

Red Sea Bottom Water. Furthermore, this contamination provides a useful tool for estimating the relative contributions of GAW and GSW to the formation of bottom water in the Red Sea, provided that the GSW outflow does not contain such an anomaly. Since the temporal input function of the pollution is unknown and observations exist only in 1999, the following study is limited to the observations in February and March 1999. It is assumed that the contamination signal has a steady source.

[34] A simple box model is implemented to estimate the range of possible GAW/GSW outflow ratios, which could produce the observed CFC saturation ratio at the bottom (below 900 m depth) of the northern Red Sea (CFC $\text{ratio}_{\text{Red Sea}}$):

$$(\text{GAW})(\text{CFC ratio}_{\text{Aqaba}})/(\text{GSW})(\text{CFC ratio}_{\text{Suez}}) \rightarrow \text{CFC ratio}_{\text{Red Sea}}$$

Because of the large concentration of the contaminated CFC-12 component in the GAW, this water mass is characterized by a ratio of the CFC-11/CFC-12 saturation (CFC $\text{ratio}_{\text{Aqaba}}$) of <1. There are no observations in the Gulf of Suez, but it is presumed that GSW did not contain a CFC-12 anomaly, which means the CFC $\text{ratio}_{\text{Suez}}$ =1. This assumption is supported by the measurements along the zonal section of the northern Red Sea. If GSW contained such a CFC-12 anomaly, one would expect a concentration maximum at the western edge of this section (Figure 2) similar to the salinity maximum, which was not observed.

[35] The water depth of the Gulf of Suez is only about 50 m, and the water column is well mixed in winter [*Soliman*, 1995]. Therefore it is assumed that the CFC concentrations in the gulf are close to equilibrium with the atmospheric values.

[36] With these assumptions and by using the contamination signal of CFC-12 it is possible to separate GSW and GAW. The objective is to get an estimate of the transport ratio of the dense inflow from both gulfs below 900 m depth, which is valid for the time period of *Meteor* cruise M44/2 (February/March 1999).

[37] The layer of bottom water in the northern Red Sea is represented by a box, which extends from 900 m to the bottom north of 27°N. In this box the CFC-12 component is initially not contaminated, and the anomaly is only introduced by the steady inflow of GAW. It is assumed that this box is completely mixed and that there is an inflow from both gulfs into the box. Because of mass conservation, the inflows of GAW and GSW force a southward outflow of mixed bottom water. No formation of deep water by open ocean convection in that region is considered.

[38] Because of the limited duration of the measurements and the lack of information about the temporal evolution of the CFC-12 anomaly, steady state is considered. However, the box model can provide some estimate of the contribu-

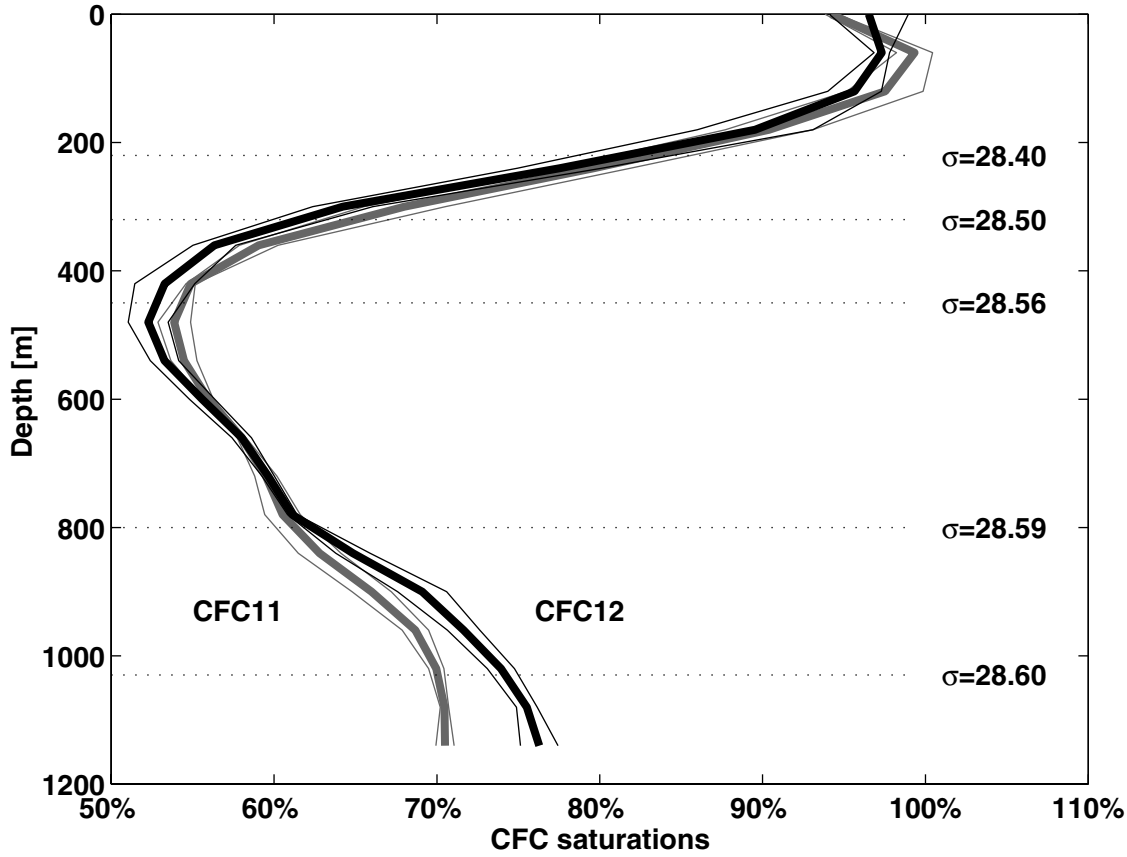

Figure 13. Profiles of the mean CFC saturation (bold lines) measured three times in the northern part of the Red Sea (station X). The thin lines represent the standard deviation. The dotted lines indicate the isopycnals.

tion of GAW and GSW to the formation of deep water for the observation period in February/March 1999.

[39] Therefore both input functions of the inflow from the gulfs into the Red Sea are constant. Because of the absence of measurements in the Strait of Tiran, the input function that characterizes the GAW outflow was chosen according to the observation made at the southern end of the gulf. During cruise M44/2 the CFC-11/CFC-12 saturation ratio north of the Strait of Tiran (station VI) had values of 0.8–0.95 within the density range of the GAW outflow ($28.6 \leq \sigma_\theta \leq 28.75$; Figure 14) [*Murray et al.*, 1984]. The measured CFC-11/CFC-12 saturation ratio in the bottom water of the Red Sea (CFC $\text{ratio}_{\text{Red Sea}}$) was about 0.93 (70% CFC-11, 75% CFC-12; Figure 13); thus for the input function of CFC $\text{ratio}_{\text{Aqaba}}$ no ratios higher than 0.93 are applied.

[40] Some experiments with CFC $\text{ratio}_{\text{Aqaba}}$ between 0.8 and 0.93 were made, keeping the GSW input ratio constant at 1.0. The chosen CFC input function determines the outflow transport ratio of Gulf of Aqaba and Gulf of Suez Water (GAW/GSW), which is necessary to simulate the observed ratio of the CFC-11/CFC-12 saturations in the Red Sea. This relationship is shown in Figure 15.

[41] The smaller the CFC ratio (the higher the CFC-12 anomaly) of the inflowing GAW, the smaller the required transport of GAW to explain the observed anomaly in the Red Sea. For a CFC ratio larger than 0.85 the transport of GAW would be stronger than the one of GSW (Figure 15). These CFC ratio values do not seem to be unrealistic for the Strait of Tiran as GAW is diluted by mixing and entrainment with the surrounding RSW.

[42] If the CFC ratio of the GAW outflow is about 0.87, which corresponds to a density $\sigma_\theta = 28.7$ at station VI in the Gulf of Aqaba (Figure 14), the GAW outflow will be 1.5 times stronger than the GSW transport (Figure 15). A

Table 1. CFC-11/CFC-12 Saturation Ratio Below $\sigma_\theta = 28.60$ or at the Bottom If the Density Was Not Reached

Station	Ratio of CFC-11/CFC-12 Saturation	Depth of $\sigma_\theta = 28.60$, m	Water Depth, m
VII	0.96–1.00	590–600	670
VIII	0.95–1.01	830–850	910
IX	0.98–1.02	...	885
X	0.90–0.94	1015–1025	1145
XI	0.91–0.94	1005–1020	1135
XII	0.97–0.99	...	805

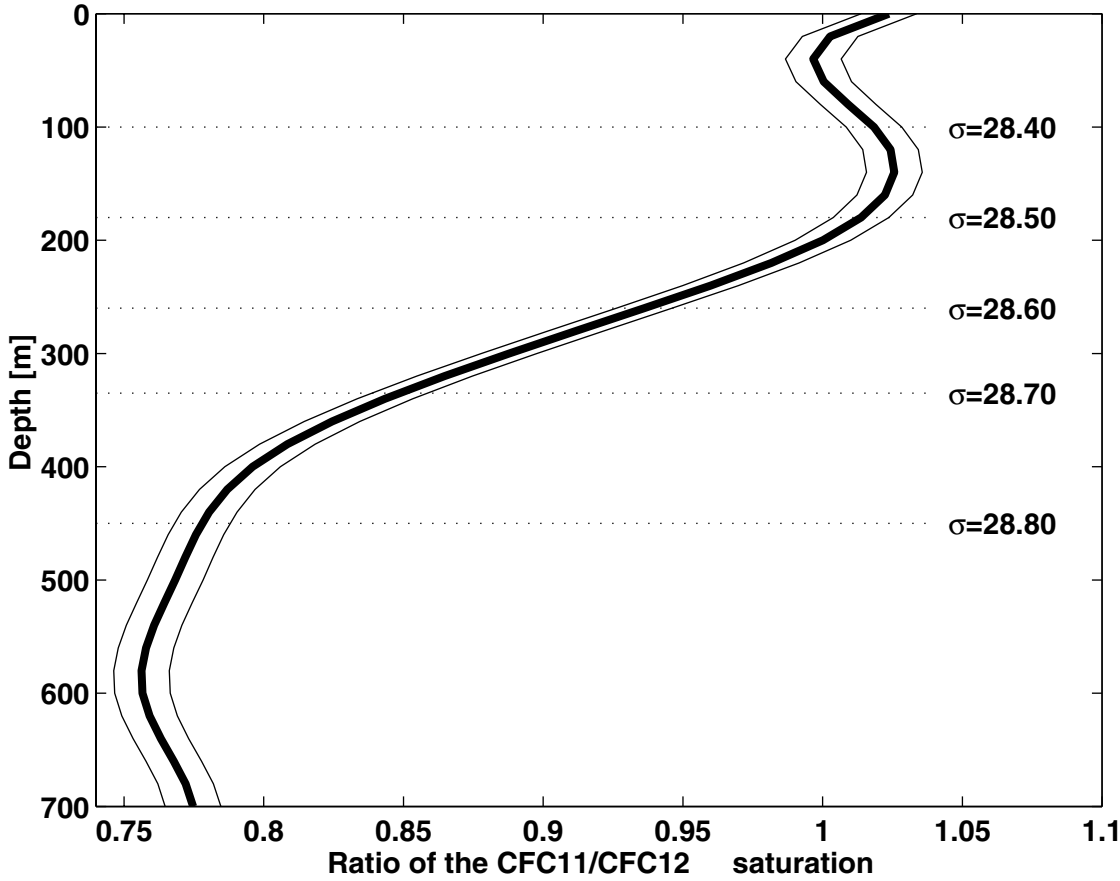

Figure 14. Mean ratio of the CFC-11/CFC-12 saturation measured north of the Strait of Tiran at station VI. The thin lines represent the standard deviation.

different CFC ratio of the GAW would have to be considered if the signal strength of the CFC-12 anomaly changes with time. For example, if the anomaly was weaker in former times, that means the CFC ratio was larger than 0.87 and the GAW outflow had to be stronger to produce the observed anomaly at the bottom of the Red Sea. However, this temporal information is not available. Nevertheless, the transport ratio of GAW/GSW shows that GAW makes a significant contribution to the formation of bottom water in the Red Sea. For comparison, the strength of the overflow from the Gulf of Aqaba is quantified in the following using direct current measurements with a vessel-mounted ADCP (VMADCP).

5.3. Transport Calculation of the GAW Outflow

[43] Direct velocity measurements in the Strait of Tiran were only carried out in winter. Therefore the (semi)annual variability of the overflow is still unknown. *Murray et al.* [1984] observed the flow field in the Strait of Tiran for the period of 1 month in February 1982 with moored current meters. The authors measured a velocity in the core of GAW of 0.5–0.75 m s^{-1} and calculated a mean outflow transport of 0.03 Sv. They observed that the core of the outflow current was located in the center of the strait, decreasing toward the side, and confirmed that the strong northerly wind exerts little effect on the mean flow. The authors also found clear evidence that the outflow was hydraulically controlled during certain phases of the spring neap tidal cycle.

[44] The estimates of the outflow transports through the Strait of Tiran from *Klinker et al.* [1976] are based on the conservation of mass, yielding about 0.07 Sv for winter and 0.045 Sv for summer. However, these estimates are questionable. For their calculations the authors used a salinity of about 41.5, which is nearly 1 higher than generally observed south of the strait.

[45] During *Meteor* cruise M44/2 the velocity field in the Strait of Tiran was measured three times with a VMADCP on along-strait sections. On each of the sections a strong southward current was observed in the lower layer with the highest current speeds of 0.8 m s^{-1} near the bottom (Figure 16). Since it was not possible to measure the density structure in both outflow regions, evidence for hydraulically controlled flow was not detectable. Because of the agreement of the VMADCP velocity profiles with the measurements of *Murray et al.* [1984], the transport in winter 1999 might be in the same range as in 1982.

[46] To satisfy the mass conservation in the Gulf of Aqaba, a northward transport of surface water from the Red Sea into the gulf of about 0.03 Sv is required. *Murray et al.* [1984] calculated a northward transport of about 0.01 Sv through the shallow Grafton Passage east of the main part of the Strait of Tiran. Thus the northward inflow through the main passage has to be more than 0.02 Sv. This is equivalent

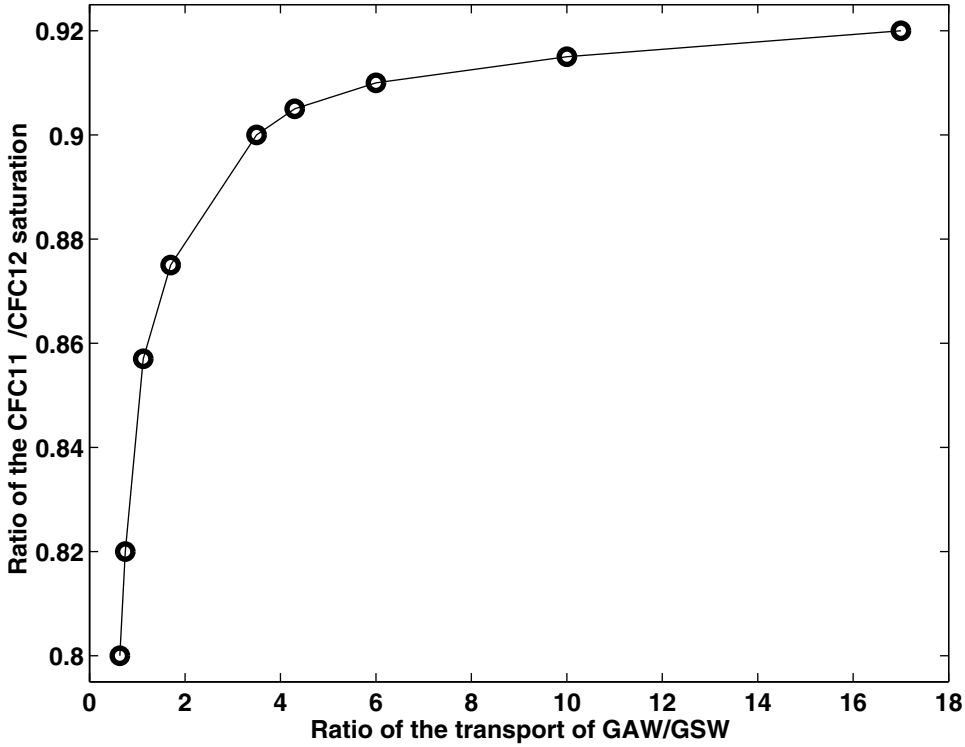

Figure 15. Ratio of the CFC-11/CFC-12 saturation in the GAW (CFC-ratio$_{Aqaba}$) versus the calculated ratio from the outflow transport of the Gulf of Aqaba and the Gulf of Suez (GAW/GSW) into the Red Sea. The circles represent the model results.

to a mean northward velocity of 0.2 m s^{-1} in the upper 100 m, which is the level of no motion chosen by *Murray et al.* [1984]. In winter 1999 the interface was found to lie between 50 and 110 m depth (Figure 16). The measured northward velocity component was smaller than 0.2 m s^{-1} during cruise M44/2, but the VMADCP did not resolve the upper 30 m of the water column. Thus the inflow into the Gulf of Aqaba might be stronger than 0.5 m s^{-1} in the upper 30 m.

6. Production Rates

[47] The published production rates and residence timescales of the deep water in the Red Sea cover a large range. The deep water was mainly defined as the water column below the oxygen minimum at 400–600 m depth, which corresponds with the observed CFC minimum (Figure 2). Former studies did not subdivide the water column into deep and bottom water.

[48] *Woelk and Quadfasel* [1996] assumed that the deep water production occurs over a period of 7 months. However, *Soliman* [1995] showed that only between January and April the density of the outflow water from the Gulf of Suez is large enough to reach down near to the bottom of the Red Sea. *Wyrtki* [1974] estimated 72 years for the residence time of the deep water. The volume of the water mass is about 1.35×10^{14} m^3. Using box models, *Eshel et al.* [1994] estimated 35 years, and *Kuntz* [1985] calculated 40 ± 20 years. *Woelk and Quadfasel* [1996] published a transport of 0.05–0.08 Sv for the formation of deep water, which results in a residence time of 40–90 years. However, they only considered the Gulf of Suez as a source of well-ventilated water.

[49] *Cember* [1988] devided the formation of new deep water into a convective mode (about 0.05 Sv) and an isopycnal mode (injection beneath the pycnocline of new deep water) with a production rate of about 0.11 Sv. The principal component of the convectively formed new deep water should be roughly a 1:1 mixture of dense winter outflow water from the mouth of the Gulf of Suez with the pycnocline water from the open northern Red Sea. The author mentioned that the outflow from the Gulf of Aqaba would be a secondary source of convectively formed bottom water. *Cember* [1988] assumed that a combination of the outflow from the Gulf of Aqaba and weak convective overturning in the northern Red Sea probably formed new deep water in the isopycnal mode.

[50] The present study shows that the deep water column has to be subdivided into the deep water marked by the salinity maximum and the bottom water, which contains the CFC-12 anomaly. This result was clarified by the model results, which show that the GAW outflow has a significant contribution to the formation of the bottom water (Figure 15). However, for the calculation of the residence time of the deep water mass the dense inflow from the Gulf of Suez has mainly to be considered.

[51] The dense outflow through the Strait of Tiran is about 0.03 Sv [*Murray et al.*, 1984]. Spreading from the strait toward the bottom of the Red Sea, the outflow water is modified by entrainment. Assuming that the bottom water originates only from the GAW outflow yields the upper entrainment rate. The most extreme saturation ratio of GAW

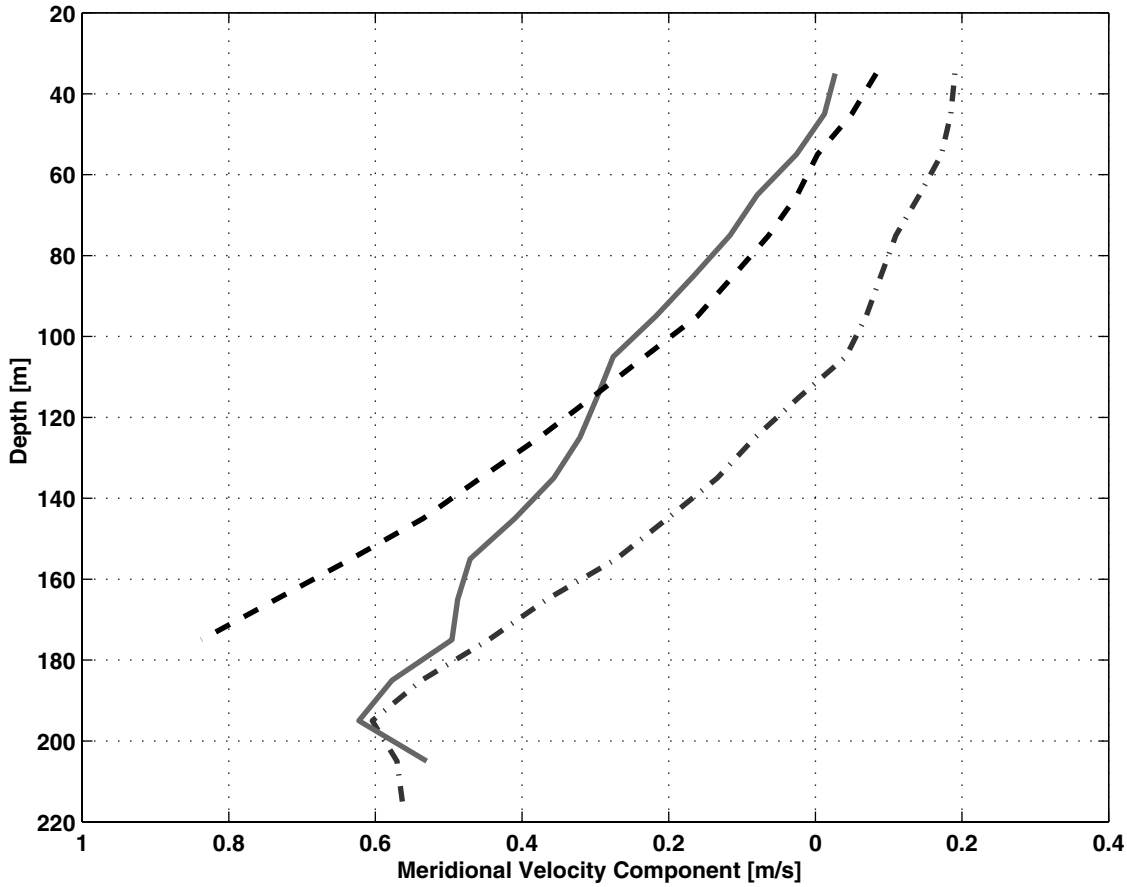

Figure 16. The along-strait component of the velocity profile at the sill of the Strait of Tiran, measured on 22 February (dot-dashed line), 26 February (solid line), and 2 March 1999 (dotted line).

in the Strait of Tiran might be 0.85 (Figure 14). Mixing this anomaly with unpolluted water to produce the observed bottom water ratio of 0.93 results in an increase of volume of 140%, which is in agreement with *Price and Baringer* [1994]. The entrainment rate will be reduced if the source ratio is larger than 0.85 or mixing with GSW is also considered.

[52] Therefore an increase of the calculated GAW outflow transport from 0.03 to 0.07 Sv by entrainment is the upper limit, which is needed to renew the bottom water. Adding the estimates from *Woelk and Quadfasel* [1996] of 0.05–0.08 Sv for the formation of deep water results in a total transport of 0.1–0.15 Sv. Thus the residence time for the volume below the oxygen minimum will be 30–45 years.

7. Summary

[53] Because of the lack of sufficiently cold and salty water masses in other regions, the deep water masses in the Red Sea can only be ventilated by water originating in the Gulf of Aqaba (GAW) and the Gulf of Suez (GSW) or by convection in the northern Red Sea. First, *Wyrtki* [1974] proposed these three sources for the formation of the deep water. However, not all of these sources were considered in some later publications, resulting in different estimates of the processes involved in the formation process. Recently, collected data during *Meteor* cruise M44/2 in February and March 1999 give, in combination with a historical data set, new insights into the formation of deep and bottom water in the northern Red Sea. The present study shows that complete mixing of the water column south of the Sinai peninsula and a renewal of the bottom water in the Red Sea due to open ocean convection is very unlikely under normal winter conditions but cannot be excluded completely for extremely cold winters. Neither the NODC data set nor the recently collected measurements with a thermosalinograph indicate SSTs that are cold enough to produce a homogeneous water column in the northern Red Sea. In all observations the SST is warmer than 22.0°C, while the temperature near the bottom is <21.3°C.

[54] Historical data show a strong seasonal cycle of the water mass characteristics in the Gulf of Suez. In winter the water column is extremely dense with values of more than $\sigma_\theta = 29.0$ (Figure 6). However, mixing with inflowing water from the Red Sea dilutes the southward spreading outflow water. The recently collected data support the observation of *Maillard* [1974] that the dense outflow from the Gulf of Suez does not exceed $\sigma_\theta = 28.6$ (Figure 7), leading to the assumption that the outflow of GSW is not dense enough to reach down to the bottom of the Red Sea. However, the available observations do not resolve the outflow characteristics completely, and it remains unclear how much of the GSW outflow enters the Red Sea closer to the coast of Egypt.

[55] *Woelk and Quadfasel* [1996] discussed that plume convection from the Gulf of Suez can also renew the deep water in the Red Sea, although their model results showed that this process is restricted to the intermediate and deep water. Below 1000 m their estimated transport is close to zero, which agrees with our result that the bottom water mass is mainly formed by the GAW outflow.

[56] In the bottom water of the Red Sea (beneath the isopycnal $\sigma_\theta = 28.59$) a CFC-12 anomaly has been observed (Figure 13), originating in the Gulf of Aqaba. This signal allows calculation of the contribution of GAW and GSW to the formation of deep water in the Red Sea for the measurement period in February/March 1999. During this period, GAW has a significant contribution. This is confirmed by estimates with a box model, which show that the GAW outflow is at least 1.5 times higher than the GSW contribution to the bottom water. However, because of the limited temporal coverage of the observations, it is not possible to make a statement about the temporal variability of the bottom water formation.

[57] In conclusion, the deep water masses in the Red Sea can be separated into two parts. The upper part is dominated be the inflow from the Gulf of Suez. Spreading into the Red Sea, it is characterized by a salinity maximum, observed at the western side of the 27.5°N section at about 900 m depth (Figure 3). The lower part is mainly formed by the dense outflow from the Gulf of Aqaba, which is marked by a CFC-12 anomaly found at the bottom of the Red Sea (Figure 13).

[58] **Acknowledgments.** We would like to thank captain and crew of the R/V *Meteor*. We acknowledge the support of M. Schütt, who performed many of the CFC analyses and thanks to A. Post for the helpful discussion on board. D. Quadfasel and S. Woelk supplied the historical data.

References

Bullister, J., and R. Weiss, Determination of CCl_3F and CCl_2F_2 in seawater and air, *Deep Sea Res., Part A*, *35*, 839–853, 1988.

Cember, R., On the sources, formation, and circulation of Red Sea Water, *J. Geophys. Res.*, *93*, 8175–8191, 1988.

Düing, W., and W. Schwill, Ausbreitung und Vermischung des salzreichen Wassers aus dem Roten Meer und aus dem Persischen Golf, *Meteor Forschungsergeb., Reihe A*, *3*, 44–66, 1967.

Eshel, G., M. Cane, and M. Blumenthal, Modes of subsurface, intermediate, and deep water renewal in the Red Sea, *J. Geophys. Res.*, *99*, 15,941–15,952, 1994.

Fine, R., M. Warner, and R. Weiss, Water mass modification at the Agulhas Retroflection: Chlorofluoromethane studies, *Deep Sea Res., Part A*, *35*, 311–332, 1988.

Gamsakhurdiya, G., S. Meshchanov, and G. Shapiro, Seasonal variations in the distribution of Red Sea Waters in the northwestern Indian Ocean, *Oceanology*, *31*, 32–37, 1991.

Hall, J., Batimetric chart of the Strait of Tiran, *Isr. J. Earth Sci.*, *24*, 69–72, 1975.

Hecht, A., and D. Anati, A description of the Strait of Tiran in winter 1978, *Isr. J. Earth Sci.*, *32*, 149–164, 1983.

Klinker, J., Z. Reiss, C. Kropach, I. Levanon, H. Harpaz, E. Halicz, and G. Assaf, Observations on the circulation pattern in the Gulf of Elat (Aqaba), Red Sea, *Isr. J. Earth Sci.*, *25*, 85–113, 1976.

Kuntz, R., Bestimmung der Tiefenwasserzirkulation der Roten Meeres anhand einer Boxmodellierung von Tritium-, He- und Salinitätsdaten, Ph.D. thesis, Ruprecht Karls Univ. Heidelberg, Heidelberg, Germany, 1985.

Maillard, C., Formation d'eau profonde en mer rouge, in *Processus de Formation des Eaux Oceaniques Profondes*, pp. 115–125, Cent. Natl. de la Rech. Sci., Verrières-le-Buisson, France, 1974.

Murray, S., A. Hecht, and A. Babcock, On the mean flow in the Tiran Strait in winter, *J. Mar. Res.*, *42*, 265–287, 1984.

Neumann, A., and D. Gill, Circulation of the Red Sea in early summer, *Deep Sea Res.*, *8*, 223–235, 1962.

Plähn, O., M. Rhein, R. Fine, and K. Sullivan, Pollutants from the Gulf War serve as water mass tracer in the Arabian Sea, *Geophys. Res. Lett.*, *26*, 71–74, 1999.

Price, J., and M. Baringer, Outflow and deepwater production by marginal seas, *Prog. Oceanogr.*, *33*, 161–200, 1994.

Rhein, M., L. Stramma, and O. Plähn, Tracer signals of the intermediate layer of the Arabian Sea, *Geophys. Res. Lett.*, *24*, 2561–2564, 1997.

Soliman, G., Hydrographic features in the Gulf of Suez and the estimation of its water and salt budgets, *Bull. Natl. Inst. Oceanogr. Fish.*, *21*, 1–33, 1995.

Woelk, S., and D. Quadfasel, Renewal of deep water in the Red Sea during 1982–1987, *J. Geophys. Res.*, *101*, 18,155–18,165, 1996.

Wolf-Vecht, A., N. Paldor, and S. Brenner, Hydrographic indications of advection/convection effects in the Gulf of Elat, *Deep Sea Res., Part II*, *39*, 1393–1401, 1992.

Wyrtki, K., On the deep circulation of the Red Sea, in *Processus de Formation des Eaux Oceaniques Profondes*, pp. 91–106, Cent. Natl. de la Rech. Sci., Verrières-le-Buisson, France, 1974.

T. H. Badewein and O. Plähn, Institut für Meereskunde, Universität Kiel, 24105, Kiel, Germany. (oplaehn@ifm.uni-kiel.de)

B. Baschek, Institute of Ocean Sciences, Sidney, B.C., Canada V8L 4B2.

M. Rhein and M. Walter, Institut für Umweltphysik, Universität Bremen, 28359 Bremen, Germany.